AN INVESTIGATION OF THE TRIPLE-SHOCK-WAVE PROBLEM

by

CHARLES E. WILSON, JR.

B.S., Kansas State University, 1962

A MASTER'S REPORT

submitted in partial fulfillment of the

requirements for the degree

MASTER OF SCIENCE

Department of Mechanical Engineering

KANSAS STATE UNIVERSITY

Manhattan, Kansas

1964

Approved by:

Major Professor

TABLE OF CONTENTS

NOMENCLATURE

a, b, c, d	- Limit points on the shock polars
A	- used to denote intersections having supersonic flow behind both reflected and Mach shocks
B	- used to denote intersections having supersonic flow behind the reflected shock and subsonic flow behind the Mach shock
C_o	- used to denote intersections having zero curvature and subsonic flow behind both reflected and Mach shocks
C_∞	- used to denote intersections having infinite curvature and subsonic flow behind both reflected and Mach shocks
c^*	- critical speed of sound
k	- ratio of specific heats
M	- Mach number
M^*	- dimensionless velocity ratio, V/c^*
P	- pressure
R, R'	- intersection points on shock polar diagram for regular reflection
S_1, S_2	- intersection points on shock polars for Mach reflection
T, T'	- used to denote triple point
V	- velocity
α	- angle between incident shock and wedge surface
α_e	- limiting angle of incidence for two shock theory
α_o	- angle of incidence at which Mach reflection is observed to begin
α'	- angle between reflected shock and wedge surface
δ	- turning angle across shock
δ_e	- turning angle beyond which regular reflection is theoretically impossible
δ_{max}	- maximum turning angle for oblique shock
θ	- flow direction
ξ	- ratio of pressure in front of a shock to that behind
μ	- viscosity

σ - angle of shock to incoming flow

χ - angle the line of travel of the triple point makes with the wall

ω - angle between the flow and the incident shock

ω' - angle between reflected shock and path of the triple point

Roman Numerals:

I - used to denote the M_1 shock polar

II - used to denote the M_2 shock polar

Subscripts:

A - signifies the incident shock

B - signifies the Mach shock

C - signifies the reflected shock

1 - signifies conditions upstream of the incident shock

2 - signifies conditions behind the incident shock

3 - signifies conditions behind the reflected shock

4 - signifies conditions behind the Mach shock

INTRODUCTION

In many practical problems, oblique shock waves are incident on fixed walls. In such cases, the shock wave is reflected, since the gas flow is assumed to follow the wall. Two types of reflection have been observed. One is known as regular reflection (Fig. 1), and is characterized by the

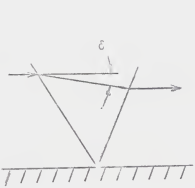

Fig. 1. Regular reflection

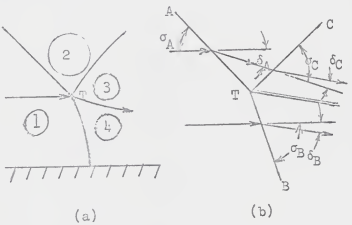

Fig. 2. Mach reflection

fact that the incident and reflected shocks intersect in a line at the wall surface. However, for all values of free-stream Mach number, there is a range of shock wave angles for which regular reflection cannot satisfy the boundary condition of parallel flow at the wall (1, 2)*. The line of intersection leaves the wall and moves out into the flow, and a third shock wave (called the Mach shock) appears, joining the wall and the line of intersection. This triple-shock phenomenon in called Mach reflection (Fig. 2). An enlarged diagram in the vicinity of the intersection is shown in Fig. 2(b).

Experimental investigation of Mach reflection has been carried out using all three of the most common optical arrangements--shadowgraph, schlieren, and interferometer. In all investigations, the axis of the optical system was been parallel to the line of shock wave intersection so that this line

*Numbers in parentheses refer to references at the end of the report.

appears as a point. Therefore, for convenience, this plane of observation has been chosen for all discussions in this report, and henceforth, the line of intersection will be referred to as the point of intersection, or the triple-point.

Interactions other than with a solid wall also may produce Mach reflection. For example, plane shocks converging at the plane of symmetry of a supersonic, 2-dimensional jet often result in a Mach reflection in the vicinity of the axis.*

The type of regular interaction in steady flow shown in Fig. 1 is impossible if the incident Mach number M_1 is too small or if the deflection angle δ is too large. In the Mach reflection which then occurs (Fig. 2), the Mach shock must be normal to the wall in the neighborhood of the wall, for otherwise, a change in flow direction would occur at the wall. Since the Mach shock is generally curved, the flow behind it is non-uniform in velocity and direction, hence, rotational. It has been observed that a fourth discontinuity trails behind the triple point. This is the slip line forming the boundary between the flow passing through the Mach shock and the flow passing through the incident and reflected shocks. The existence of the slip line is consistent with theoretical considerations of the problem, since fluid passing through the incident and reflected shocks undergoes a smaller change in entropy than that passing through the Mach shock. Since the total energy is the same on the two sides of the slip line and since the static pressure must be the same, the density and velocity are greater above this boundary while the temperature is greater below. The reflected shock as well as the Mach shock can be curved; thus the flow behind the reflected shock can also be rotational.

*Also, a conical shock convergent at the axis of a supersonic, axially symmetric jet always results in a Mach reflection in the vicinity of the axis. (See Reference 5)

An analogous reflection pattern may be observed in a shock tube when the incident shock wave hits a straight wedge as shown in Fig. 3. This pattern may be transformed to a pseudo-stationary case similar to Fig. 2 by choosing a frame of reference in which the triple point is at rest. The free stream flow M_1 is in the direction TO and ω is the angle of the incident wave.

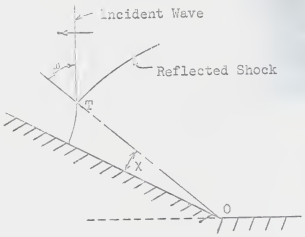

Fig. 3. Mach reflection in the shock tube.

The purposes of this report are:

(1) to present the classical "perfect fluid" solution of the triple-shock problem;

(2) to perform some typical numerical solutions using this classical theory;

(3) to compare this theory with experimental results; and

(4) to discuss and evaluate the various theories that have been advanced to explain the discrepancies between the classical theory and experimental data.

THE BASIC EQUATIONS AND THEIR SOLUTION

Von Neumann (4) and Oggink (5) independently developed the first solutions of the triple-shock problem. Their method will be referred to as the "simple" theory, although, from a mathematical point of view, this is surely a misnomer. Their idea was to consider the fluid to be non-viscous, non-heat-conducting, non-radiating, of constant chemical composition; and to replace each shock wave by a plane, disregarding any possible curvature of the shocks and any possible finite shock wave thickness. Under those assumptions, they examined boundary compatibility downstream of the triple point. Combinations of plane and reflected shocks must be found which produce the same static

pressure and flow direction in the two domains downstream of the triple-point. In terms of Fig. 2(b):

$$P_4 = P_3$$

or

$$\frac{P_4}{P_1} = \frac{P_2}{P_1}\frac{P_3}{P_2}$$

and

$$\delta_B = \delta_A + \delta_C$$

Unfortunately, no convenient explicit algebraic relations exist for the oblique shock when M_1 and δ are taken as independent parameters.* However, the following relations exist when M_1 and σ are chosen as the parameters (3, 7). In each of the following pairs of equations, the second form of the equation applies for $k = 1.4$:

$$\frac{P_2}{P_1} = \frac{2kM_1^2\sin^2\sigma_A - (k-1)}{k+1} = \frac{7M_1^2\sin^2\sigma_A - 1}{6}$$

$$\cot\delta_A = \left[\frac{(k+1)M_1^2}{2(M_1^2\sin^2\sigma_A - 1)} - 1\right]\tan\sigma_A = \left[\frac{1.2\,M_1^2}{M_1^2\sin^2\sigma_A - 1} - 1\right]\tan\sigma_A$$

Similar equations can be written which express $\frac{P_3}{P_2}$, $\frac{P_4}{P_1}$, $\cot\delta_B$, and $\cot\delta_C$ in terms of M_1, M_2, σ_A, σ_B, and σ_C. Now since

$$\delta_B = \delta_A + \delta_C$$

$$\cot\delta_B = \cot(\delta_A + \delta_C)$$

applying a trigonometric identity:

$$\cot\delta_B = \frac{\cot\delta_A\cot\delta_C - 1}{\cot\delta_A + \cot\delta_C}$$

*Computational charts are available which relate M_1, σ, and δ (6,7,8).

Also,

$$M_2^2 = \frac{(k+1)M_1^4\sin^2\sigma_A - 4(M_1^2\sin^2\sigma_A - 1)(kM_1^2\sin^2\sigma_A + 1)}{[2kM_1^2\sin^2\sigma_A - (k-1)][(k-1)M_1^2\sin^2\sigma_A + 2]}$$

$$= \frac{36M_1^4\sin^2\sigma_A - 5(M_1^2\sin^2\sigma_A - 1)(7M_1^2\sin^2\sigma_A + 5)}{(7M_1^2\sin^2\sigma_A - 1)(M_1^2\sin^2\sigma_A + 5)}$$

Then, using these expressions, the compatibility equations become

$$\frac{2k}{k+1}M_1^2\sin^2\sigma_B - \frac{k-1}{k+1} = \left[\frac{2kM_1^2\sin^2\sigma_A - (k-1)}{k+1}\right]\left[\frac{2kM_2^2\sin^2\sigma_C - (k-1)}{k+1}\right]$$

$$7M_1^2\sin^2\sigma_B - 1 = \frac{1}{6}(7M_1^2\sin^2\sigma_A - 1)(7M_2^2\sin^2\sigma_C - 1)$$

and

$$\left[\frac{(k+1)M_1^2}{2(M_1^2\sin^2\sigma_B - 1)} - 1\right]\tan\sigma_B = \frac{\left[\frac{(k+1)M_1^2}{2(M_1^2\sin^2\sigma_A - 1)} - 1\right]\left[\frac{(k+1)M_2^2}{2(M_2^2\sin^2\sigma_C - 1)} - 1\right]\tan\sigma_A\tan\sigma_C - 1}{\left[\frac{(k+1)M_1^2}{2(M_1^2\sin^2\sigma_A - 1)} - 1\right]\tan\sigma_A + \left[\frac{(k+1)M_2^2}{2(M_2^2\sin^2\sigma_C - 1)} - 1\right]\tan\sigma_C}$$

$$\left(\frac{1.2M_1^2}{M_1^2\sin^2\sigma_B - 1} - 1\right)\tan\sigma_B = \frac{\left(\frac{1.2M_1^2}{M_1^2\sin^2\sigma_A - 1} - 1\right)\left(\frac{1.2M_2^2}{M_2^2\sin^2\sigma_C - 1} - 1\right)\tan\sigma_A\tan\sigma_C - 1}{\left(\frac{1.2M_1^2}{M_1^2\sin^2\sigma_A - 1} - 1\right)\tan\sigma_A + \left(\frac{1.2M_2^2}{M_2^2\sin^2\sigma_C - 1} - 1\right)\tan\sigma_C}$$

There are five variables in these two equations: M_1, M_2, σ_A, σ_B, σ_C. In most problems the incident Mach number M_1 and one of the shock wave angles, σ_A or σ_B, will be known. In the case where M_1 and σ_A are known, M_2 may be calculated at once. Thus, the compatibility equations reduce to two equations in the remaining two unknowns, σ_B and σ_C. However, because of the complexity of the equations, direct solution is impossible.

There are several ways to solve the problem. One straight-forward method, which is especially suitable if one has a rough idea of the values of σ_B and/or σ_C, is the trial-and-error solution. A value of σ_C, for example,

is assumed. From the pressure equation σ_B is calculated; these values of M_1, σ_A, and σ_B are then substituted into the deflection equation. If the left hand member and the right hand member turn out to be equal, the originally assumed value of σ_B was correct. If the two members turn out unequal, a new value of σ_B is assumed, and the procedure repeated until a check is obtained in the deflection equation.

If, originally, σ_B were known instead of σ_A, the problem is somewhat more difficult to solve, for now M_2 is not known a priori. Again, trial-and-error may be employed--this time, for three equations in three unknowns.

Early workers discovered a second method of solution which was graphical (5, 9). Because of the pressure and flow direction requirements, it is obvious that the solution must be given by the intersection of two shock wave polar diagrams plotted in P - δ coordinates. The shock polar in P - δ coordinates is a heart-shaped curve, (see Fig. 4), on which the states of the Mach shock and incident shock are located. M_2 is determined as shown above.

Fig. 4. Construction of the solution

Corresponding to M_2 is a second shock polar which may be drawn right on top of the polar for M_1 with the initial point of the M_2 polar displaced along the M_1 polar by the angle δ_A. The point of intersection 3,4 of the polars is the required solution. Depending on the values of M_1 and δ_A, there may be one point of intersection, two points, or none at all (excluding the initial point 2). Feink showed that, using the assumption stated in the first of this section, the M_2 polar lay entirely in the interior of the M_1 polar for $M_1 < 1.245$, and that hence, no intersection

of the polars occurred. He did this by calculating the direction of the tangent to both polar curves at the starting point of the M_2 polar. (The tangent is found by differentiating the equation relating δ and P.) Eggink found that there is a limiting point below all values of M_1, beyond which the M_2 polar lies entirely inside the M_1 polar. Moreover, he found that there was no value of δ for which any part of the M_2 polar lay outside the M_1 polar for $M_1 < 1.245$. The fact that the Mach configuration is observed experimentally for $M_1 < 1.245$ exposes the first short-coming of the so-called simple theory.

The limiting case mentioned above may be seen to be the case when the reflected shock is of vanishing intensity (a Mach wave), and the incident and Mach shocks are on the same straight line. Of course, a second limiting case in the physical phase occurs when the incident shock has vanishing intensity, and the Mach and "reflected" shocks are just one continuous oblique shock. This case is illustrated in the P - δ polar (Fig. 5). As $\delta \to 0$, the solution point 3,4 approaches the limiting point, a.

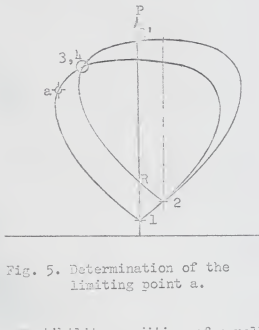

Fig. 5. Determination of the limiting point a.

It should be pointed out that such a configuration as illustrated in Fig. 5 (termed inverted Mach configuration) in which the M_2 polar crosses the P axis of the M_1 polar, is an unstable solution to the problem of shock reflection at a wall (2). The inverted Mach reflection would be destroyed, and regular reflection could appear in its place, since the compatibility condition of parallel flow at the wall can now be satisfied

by the M_2 polar at two different points (R and R', in Fig. 5). Here, then, we have, illustrated in the P - δ polars, the condition for the end of regular reflection and the onset of Mach reflection. The further point 2 is displaced from point 1 in Fig. 5, the smaller the second polar becomes, until finally it shrinks to a point at the sonic point on the M_1 polar. Clearly, then, the intersection points, R and R', disappear for δ greater than some δ_e . This should mark the beginning of Mach reflection (17).

Ehrlink found that the polars intersect in two points, S_1 and S_2, for $M_1 > 2.55$ (Fig. 6). S_1 and S_2 run out from limiting points, a and c. S_1 varies from a to the limiting point b, as before. The second intersection point S_2 starts at c and advances to d as δ increases; when S_2 reaches d, it is coincident with the starting point 2 of the M_2 polar. For larger δ , there is only one solution, S_1.

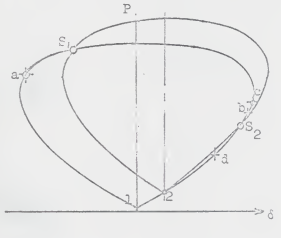

Fig. 6. Case of 2 solutions.

Graphical representations of numerical solutions have been presented in two different forms (9). One uses the shock wave angle of the Mach shock, σ_B , and M_1^* as coordinates with the angle of incident shock, σ_A , as a parameter. This representation shows that, in the region where $M_1 > 2.55$, there is a range of incident shock wave angles, σ_A , for which there are two solutions for σ_B , etc. Moreover, for $M_1 > 3.26$, there is a certain range of σ_B in which the solutions, S_1 (which is single valued) and S_2 (which is double valued) overlap; under those conditions three possible solutions for σ_A , etc. exist. Another observation of interest is that there is a small region of solutions for all values of M_1, in which flow is supersonic behind both the Mach and the reflected shocks.

When one is principally interested in angles of deflection, the second representation is advantageous. It presents δ_A and δ_B as rectangular coordinates with M_1^* as parameter. For $M_1 > 3.72$, the curves for the S_2 solution have a point of inflection, so that there are four distinct solutions associated with one value of δ_B, for δ_B between limit point b and δ_{max}.

Eggink extends the hodograph shock polar diagram (Fig. 7) to present his results. This representation has the advantage that the shock wave angle, angle of deflection, and all Mach numbers can be read directly.

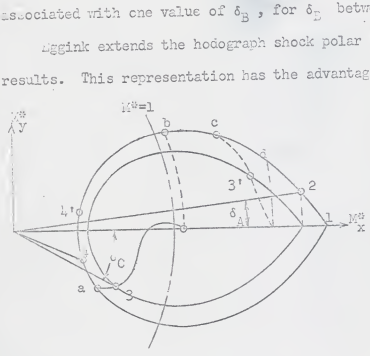

Fig. 7. The shock-polar diagram for a triple shock.

Eggink plotted solutions for a number of values of M_1^*. For each M_1^*, he found δ_C (and thereby point 3 in the hodograph of Fig. 7) from the intersection of the P - δ shock polars. The points 3 are computed as the M_2^* polar is allowed to move along the fixed M_1^* polar through all permissible values of M_2^*. The points 3 are then plotted on the variable hodograph polars M_2^* and joined (Fig. 7) by a curve. The curves begin at the limiting point a or c on polar M_1^* and end on the axis of the diagram at the M^* that corresponds to limiting points b and d. Thus, one can start with a given M_1^* with which a definite shock polar is associated. The incident shock is determined by prescribing δ_A, and M_2^* is obtained. The M_2^* hodograph polar is rotated back by the angle δ_A about O as a center, so that the initial point 2 lies on the M_x^* axis. Point 3 is located by the intersection of the M_2^* polar and the locus of points 3

appropriate to the given M_1*. Thus, M_3* and δ_C are determined. Finally, point 4 is found on the M_1* polar by using the compatibility equation $\delta_D = \delta_A + \delta_C$. A case is illustrated in Fig. 7 which has two solutions. The second solution, when one exists, is given by the dashed locus of points 3'.

The simple theory interactions may be divided into three groups. Group A is the case when flow on both sides of the slip line is supersonic. Group B contains those cases when flow behind the reflected shock is supersonic and that behind the Mach shock is subsonic. Group C has subsonic flow on both sides of the slip line.

SAMPLE SOLUTIONS USING THE SIMPLE THEORY

In this section sample solutions are presented for all three groups of simple-theory interactions. The trial-and-error approach will be used to solve the equations directly, and this method then will be checked by use of the various computational curves available (6,7,8) as well as the charts presented in References 5 and 9.

GROUP A: supersonic-supersonic

Given : $M_1 = 1.557$ $\sigma_B = 60°$

Solution: $M_4^2 = \dfrac{36(2.426)(1.8173) - 5(0.8193)(12.735+5)}{11.735(6.8193)}$ $\qquad M_4 = 1.038$

or $\delta_3 = 1.7321\left[\dfrac{1.2(2.426)}{0.8193} - 1\right] = 4.422$ $\qquad \delta_C = \theta_3 = \theta_4 = 12°45'$

Assume $\sigma_A = 53°15'$, $\qquad M_2^2 = \dfrac{36(2.426)1.6376 - 5(0.6376)16.4632}{10.4633(6.6376)} = 1.302$

$\sigma_A = 67°3'$. Now check the assumption by calculating cot δ_B

or $\delta_B = \dfrac{1.4415\left[1.2\left(\frac{2.426}{0.6376}\right) - 1\right] + 2.361\left[1.2\left(\frac{1.7022}{0.1044}\right) - 1\right]}{1.4415(3.565) + 2.361(14.405)} = 4.422$

This is in agreement with the known value, so our assumed value of σ_A must be correct.

$\delta_A = \theta_2 = 11°00'$ $\quad M_2 = 1.141$ $\quad M_3 = 1.048$

Using the computation curves, the following values are obtained:

$M_2 = 1.146$ $\quad M_3 = 1.052$ $\quad M_4 = 1.038$

$\theta_2 = \delta_A = 10°57'$ $\quad \delta_B = \theta_3 = \theta_4 = 12°44'$ $\quad \sigma_A = 55°6'$ $\quad \sigma_c = 66°36'$

GROUP B : supersonic-subsonic

Given : $M_1 = 2.86$ $\quad \sigma_A = 47.5°$

Solution : $M_2^2 = \dfrac{36(8.180)4.446 - 5(3.446)36.12}{30.12(9.446)}$ $\quad M_2 = 1.554$

Assume $\sigma_c = 57°48'$ $\quad 7M_1^2 \sin^2\sigma_B - 1 = 5.021\left[7(1.7283)-1\right]$

$\sin \sigma_B = 0.99531$ $\quad \sigma_B = 84°27'$

The assumption is checked by calculating the value of both members of the deflection equation. The left hand member is denoted as D_1, and the right hand member as D_2.

$D_1 = 0.3819 \tan 84°27' = 3.930$

$$D_2 = \frac{(2.848-1)\left(1.2\left(\frac{2.414}{0.7283}\right)-1\right)\tan 47.5° \tan 57.8° - 1}{1.8482 \tan 47.5° + 2.977 \tan 57.8°} = 3.887$$

The two members are in close agreement, so the assumed value of σ_c is correct.

$M_2 = 1.554$ $\quad M_3 = 1.0685$ $\quad M_4 = 0.5156$

$\sigma_B = 84°27'$ $\quad \sigma_c = 57°48'$

$\delta_A = \theta_2 = 26°22'$ $\quad \delta_B = \theta_3 = \theta_4 = 14°26'$

Using Eggink's shock polar diagram, the following values are obtained:

$M_2 = 1.5575$ $\quad M_3 = 1.086$ $\quad M_4 = 0.5055$

$\delta_A = \theta_2 = 26°36'$ $\quad \delta_c = 12°$ $\quad \delta_B = \theta_3 = \theta_4 = 14°30'$

Using the computation charts, these values are obtained:

$M_2 = 1.545$ $M_3 = 1.085$ $M_4 = 0.520$ $\sigma_B = 84°18'$

$\delta_A = \theta_2 = 26°24'$ $\delta_B = \theta_3 = \theta_4 = 14°42'$ $\sigma_c = 57°54'$

GROUP C : subsonic-subsonic

Given : $M_1 = 1.732$ $\sigma_A = 49°$

Solution : $M_2^2 = \dfrac{36(3)1.7087 - 5(0.7087)16.961}{10.961(6.7087)}$ $M_2 = 1.301$

Assume $\sigma_c = 95°36'$ $7M_1^2 \sin^2\sigma_B - 1 = 1.8268 \left[7(1.6760) - 1\right]$

$\sin \sigma_B = 0.99053$ $\sigma_B = 82°6'$

$D_1 = 0.85223 \tan 82°6' = 6.149$

$$D_2 = \frac{4.08\left[1.2\left(\frac{1.6922}{0.6760}\right) - 1\right]\tan 49° \tan 95°36' - 1}{4.08 \tan 49° + 2.006 \tan 95°36'} = 6.156$$

This constitutes a reasonable check, so the assumed σ_c is correct.

$M_2 = 1.301$ $M_3 = 0.7973$ $M_4 = 0.6661$

$\sigma_B = 82°6'$ $\sigma_c = 95°36'$

$\delta_A = \theta_2 = 12°$ $\delta_B = \theta_3 = \theta_4 = 9°14'$

The values obtained from the computation charts are :

$M_2 = 1.300$ $M_3 = 0.810$ $M_4 = 0.670$

$\sigma_B = 82°$ $\sigma_c = 95°42'$

$\delta_A = \theta_2 = 12°$ $\delta_B = \theta_3 = \theta_4 = 9°12'$

It was observed that the trial-and-error solution used to solve the supersonic-supersonic case (Group A) was more difficult than the other cases because of the decision to match values of cot δ_B . As δ_B turned out to be quite small, the process was extremely non-linear, and interpolation and extrapolation was inaccurate, even for variations of only 0.1° in angle. However, when the check was made using computational curves, it was decided to match values of pressure ratio, and this procedure was much more easily applied.

EXPERIMENTAL RESULTS

Most of the experimental work has been done in the shock tube rather than in the wind tunnel. The plane shock wave is incident on a plane rigid wall which makes an angle α with the shock. This angle and the shock strength $\xi = \frac{P_1}{P_2}$ are convenient parameters to describe the results of these experiments. In air, regular reflection occurs for small α at all values of ξ (10, 11, 12).

Holding $\xi = \xi_1 =$ constant, we note that regular reflection occurs as α increases from 0° up to some angle α_o , at which point the point of inter-

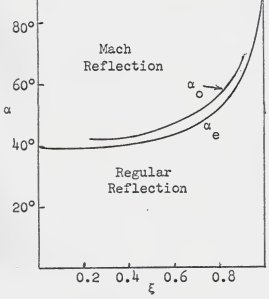

Fig. 8. Regions of regular and Mach reflection

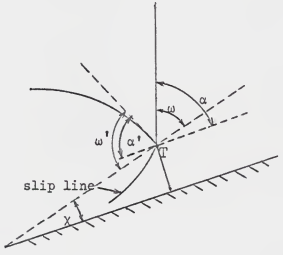

Fig. 9. Notation of angles used in Mach reflection

section pulls away from the wall and Mach reflection ensues. All experiments (10, 13) show that this angle α is 2° to 3° beyond the theoretically predicted extreme angle for regular reflection α_e (Fig. 8). Although the difference is small, it has been consistently noted by independent experimenters and cannot be explained as experimental error, since α can be measured quite accurately. In presenting data on Mach reflection it is convenient to give angles with respect to the line joining the triple-point and the corner T0. The angle between line T0 and the wall is χ. The incident shock I and the reflected shock R of Fig. 9 make angles ω and ω', at the triple point with T0. Also,

$$\omega = \alpha - \chi \qquad\qquad \omega' = \alpha' + \chi$$

A comparison of experiment and theory, from Reference 10, is shown in Fig. 10. Data are for two shock strengths, $\xi_1 = 0.8$ and $\xi_2 = 0.2$, representing weak and strong shocks respectively. For strong shocks, agreement in Mach reflection region is not bad, but certainly not as good as for regular reflection. The deviations are consistent and above any normal experimental error (10). For weak shocks, there is a large discrepancy.

Another feature to be pointed out in Fig. 10 is that for weak shocks, Mach reflection seems to join on smoothly where regular reflection stops while for strong shocks there is a sharp discon-

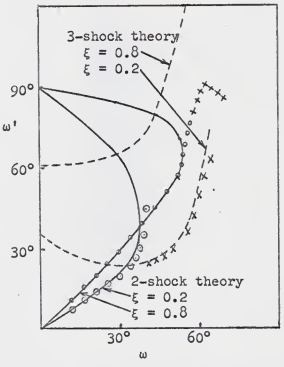

Fig. 10. Comparison of theory and experiment

tinuity in ω' when Mach reflection begins as is predicted by the simple theory. In all cases, regular reflection persists beyond the theoretical limit; this persistence is in very obvious disagreement with the simple theory in the case of weak shocks. Here, then, is strong evidence showing the inadequacy of the simple theory.

DISCUSSION AND CONCLUSIONS

The first discrepancy noted was the fact that the simple theory predicted no triple-shock solutions for $M_1 < 1.245$, whereas the configuration is observed experimentally for all supersonic M_1. It will be recalled that the reason the simple theory predicted no solution was the two polars had no intersection in the P - δ plane. The gap in the theory was filled by Guderley (14) who found a theoretically correct way of inserting a Prandtl-Meyer expansion at the triple point. Guderley's analysis is restricted to weak shocks, where entropy changes through the shocks may be neglected.

The general character of a Guderley solution is shown in the physical and hodograph planes in Fig. 11. An enlarged diagram of the hodograph in

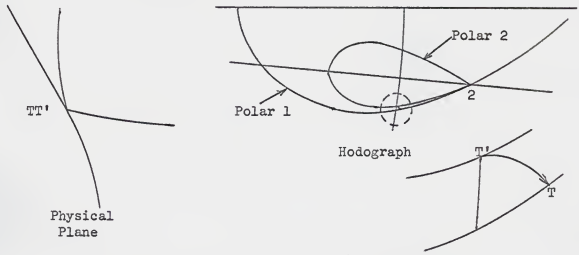

Fig. 11. Guderley's triple shock wave solution

the vicinity of the triple point is also shown. The reflected shock at the triple point is given by point T' which is the intersection of sonic line with polar II.. A Prandtl-Meyer expansion centered at the triple point is inserted in the flow behind the reflected shock, hence the streamline from T' in the hodograph follows a characteristic curve T'T. The point T is the intersection of the characteristic with polar I, and gives the location of the Mach stem in the hodograph.

Unfortunately, Guderley's new solution still seems to disagree widely with experiment for weak shocks. One possible explanation for this apparent failure of the theory is that in the experiments the shock angles have not been measured sufficiently close to the triple point to be compared with theory. It is observed that both the reflected shock and Mach stem are curved as they approach the triple point. The experimental photograph is always blurred in a small region arround the triple point, and, possibly, the shock waves are highly curved in this region.

The pseudo-stationary case of nearly glancing incidence in a shock tube may be simplified by a linearization process developed by several workers and discussed in Reference 11. Unfortunately, this simplification is of no use in the present problem. Inherent in the linearization is the requirement that the reflected shock have zero strength at the triple point, which is not the case in our problem.

Sternberg (15) has shown, in one of the most recent and extensive examinations of this problem, that the shocks are so strongly curved near the triple point in Guderley's solution that it would be impossible to observe the theoretical intersection angles, even with the best available experimental technique. Sternberg therefore concluded that the comparisons which earlier workers had made between experiment and theory were not valid

and that no one up to that time had conclusively proved that the theory was wrong. He then attempted to use a different comparison to show that the theory was incorrect.

The theories of von Neumann, Eggink and Guderley are all based on the assumption that viscosity is not a factor in establishing boundary conditions at the triple point. The simple theory of von Neumann and Eggink explicitly states that, at least in a close neighborhood of the triple point, the shocks are straight and that they separate regions of uniform flow.

Along the shock polars in the $P - \delta$ plane, the streamline slopes are fixed by the equations of motion and the Rankine-Hugoniot equation providing shock-wave curvatures are finite. In general, the streamline slopes on the intersecting polars differ at the triple point. Since the streamline from the triple point cannot have two different slopes at the same point, the shocks cannot have finite curvature at the intersection, and the triple point must be singular. If the streamlines on the two polars converge toward each other at the intersection point, the shock curvature $\rightarrow \infty$ in the physical plane. By contrast, if they diverge, the shock curvature $\rightarrow 0$ (14). By examining the simple-theory interactions, it is found that both types (convergent and divergent) of contradictions occur. Guderley showed that in his solution, also, streamline slope discontinuities occur and that, in his solution, the shock curvature must $\rightarrow \infty$ at the triple point.

It will be remembered that the simple theory interactions were classified into three groups according to flow conditions downstream of the triple point. It has been shown that when flow is supersonic behind the reflected shock (groups A and B), curvature must be zero at the triple point (16).

Group C has subsonic flow above and below the slip line just downstream of the triple point. There are two sub-groups depending on whether curvature is zero or infinite. The case in which a Group C interaction has infinite curvature, here denoted as Group C_∞, is found at all Mach numbers M_1. The sub-group having 0 curvature, denoted as Group C_0, contains the limited range of intersections on the P - δ polar that fall on the reflected shock polar between the sonic point and the point of maximum deflection. (See Fig. 12)

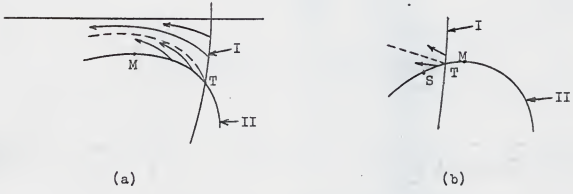

Fig. 12. Types of triple shock wave intersections

It should be noted that the intersection point in Fig. 12 (a) is on the strong shock part of polar II, while in Fig. 12 (b) it is on the weak part. When the so-called "stationary Mach reflection" (in which the Mach stem is a straight shock normal to the wall) appears, the intersection point T coincides with the point of maximum deflection M in polar II at $\delta = 0$ of polar I. The conditions for stationary reflection, as predicted by the simple theory, are $M_1 = 3.203$, $\xi = 0.433$, and hence, $\alpha = 41.5^\circ$. (17) Thus, Group C cases are found only for M_1 greater than about 3.2 in a supersonic flow or for shock pressure ratios, ξ, less than 0.433 in the shock tube.

At the transition from regular reflection to Mach reflection, one should be able to distinguish between Groups C_o and C_∞ by observing the change in angle of the reflected shock if transition occurs as theory predicts. For Group C_o, the reflected shock angle ω' should decrease discontinuously, while for Group C_∞, it should show a sudden increase, because the intersection point T lies on different branches of the M_2 polar in the two different cases.

Recalling the discussion of experimental results in the last section, we find agreement with the prediction that ω' has a sudden decrease for Group C_o, the case of strong shocks. However, experiment shows a nearly continuous transition for the weak incident shock (Group C_∞), thus violating the theory. It is also found in experiment that the boundary between discontinuous and continuous transition is approximately $\xi = 0.42$. This compares well with the theoretically predicted value above.

We begin to suspect that there is some connection between the experimental inconsistencies and the character of Group C_∞ of Fig. 12 (a). Several streamlines are shown therein and the dotted line of this same figure is the slip line. A well established theorem of the hodograph plane due to Busemann states that, in subsonic flow, a region in the hodograph with crowded streamlines corresponds to nearly uniform flow in the physical plane, while a region with few streamlines in the hodograph is associated with a narrow field of rapidly changing flow. Using this theorem, it has been argued (17) that the quantities measured experimentally are those at point M and not those at the actual triple point T in Fig. 12 (a). If this were the case, a seemingly continuous transition would take place if the flow behind the reflected shock is subsonic.

Actually, infinite curvatures in a real gas are impossible, and viscosity

should be considered to see if it has any effect on the solution. Sternberg appears to be the only author to date who has investigated the significance of viscous forces. He first shows that if excessive curvature is the only modification of the "perfect fluid" solutions needed, then viscosity is not important. As a general rule, it has been shown that the weaker the shock wave, the thicker it is (18). So Sternberg chose a weak shock ($\xi = 0.8$) to obtain a relatively thick shock wave (on the order of 3×10^{-4} cm at ordinary atmospheric conditions). As long as radii of curvature were 100 times this value, or 3×10^{-2} cm, curvature should not affect our use of shock polars as boundaries in the hodograph. Using an electric tank analogy, he shows that curvature is not a factor except within less than 0.1 mm of the triple point and is thus unobservable in the experiments.

Sternberg next attempted to show that viscosity fundamentally alters the boundary conditions at the intersection. Using an analysis contained in Reference 18, he calculated distributions of pressure and temperature along a streamline within each of the three shocks and showed that there are significant differences of pressure, temperature, and direction within the waves along the dividing streamline. This, he argued, justified the choice of a non-Rankine-Hugoniot zone of transition between the incident and reflected shocks on the one side, and the Mach shock on the other. He asserted that within this zone there would be significant pressure and temperature gradients along the front, as well as normal to it. Hence, the structure would be 2-dimensional, and would not conform to the one-dimensional Rankine-Hugoniot (R - H) equations. It follows from this conclusion of Sternberg that the boundary conditions for Group C of the perfect fluid solutions are fundamentally inconsistent when applied to a real fluid.

Sternberg then tried to justify his theory that a non-R - H zone

separates the three R - H shocks by constructing a model to replace perfect fluid solutions of Group C_∞ and performing a sample calculation using his model. Salient features of the model are now described. It is assumed that pressure and direction vary significantly along the downstream edge of the non-R - H zone (See Fig. 13), i.e., $P_C > P_E$ and $\theta_C \neq \theta_E$. Viscosity is finite, and the Navier-Stokes equations apply. The flow field is now described in the vicinity of the intersection, by selecting reasonable values for shock wave angles at the edge of the non-R - H zone. From this point in his discussion, Sternberg advanced what seems to this author to be a questionable discussion about what a "reasonable" value of the reflected shock wave angle would be. The available experimental data suggest a value of 95° for the choice of incident conditions which he selects. But Sternberg abandons the data and suggests that any value greater than 90° is "physically impossible" since this implies that the reflected shock runs upstream from the triple point. It has been pointed out that it seems unreasonable to dismiss the considerable amount of both wind tunnel and shock tube evidence that do show flows incident as much as 105° to that shock front (19). Sternberg seems to overlook the fact that, since flow is subsonic downstream of the reflected shock, signals from downstream disturbances can reach the reflected shock. In particular, the effects of a curving slip line will be impressed on the reflected shock and will affect its shape. However, it must be acknow-

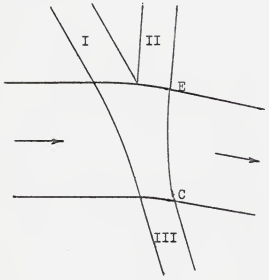

Fig. 13. Sternberg's proposed real fluid model in the physical plane.

ACKNOWLEDGEMENT

The author would like to express his deep gratitude to Dr. J. M. Bowyer, Jr. who has given patient guidance and encouragement throughout the work on this report.

REFERENCES

1. Shapiro, A. H.
"The Dynamics and Thermodynamics of Compressible Fluid Flow", Vol. I, The Ronald Press Company, New York, (1953), pp. 553-558.

2. Courant, R. and K. O. Friedrichs
"Supersonic Flow and Shock Waves", Interscience Publishers, Inc., New York, (1948), pp. 331-350.

3. Bowyer, J. M., L. D'Attorre, and H. Yoshihara.
"The Flow Field Resulting from Mach Reflection on a Convergent Conical Shock at the Axis of a Supersonic, Axially Symmetric Jet", Report GDA 63-0586, General Dynamics/ Astronautics, San Diego, California, (July, 1963)

4. von Neumann, J.
"Oblique Reflection of Shocks", Explosives Research Report No. 12, Bureau of Ordnance, U. S. Navy Department, (1943).

5. Eggink, H.
"Compression Shocks of Detached Flow", NACA Tech. Memo. 1150. Transl. from "Zentrale für wissenschaftliches Berichtswesen der Luftfahrtforschung des Generalluftzeugmeisters (ZWB) Berlin-Adlershof, Forshungbericht 1850," Aachen, Germany, (August 1943).

6. Dailey, C. L. and F. C. Wood
"Computation Curves for Compressible Fluid Problems", John Wiley & Sons, Inc., New York, (1949).

7. Ames Research Staff
"Equations, Tables, and Charts for Compressible Flow", NACA Report 1135, (1953).

8. Neice, M. M.
"Tables and Charts of Flow Parameters Across Oblique Shocks", NACA TN 1673, (August 1948).

9. Schäfer, M.
"Method of Characteristics and Shock Waves", Article 4.1 of "Flows of Compressible Fluids", W. Tollmein (Editor). Translated from AVA (Aerodynamische Versuchsanstalt Göttingen) Monographs" by British M. A. P. Völkenrode Reports and Translations #996", (May, 1948), pp. 31-36.

10. Bleakney, W., and A. H. Taub.
"Interaction of Shock Waves", Reviews of Modern Physics, Vol. 21, No. 4, (October, 1949), pp. 584-605.

11. Fletcher, C. H., A. H. Taub, and W. Bleakney
"The Mach Reflection of Shock Waves at Nearly Glancing Incidence", Reviews of Modern Physics, Vol. 23, No. 3, (July, 1951), pp. 271-286.

12. Jahn, R. G.
"Transition Processes in Shock Wave Interactions", J. of Fluid Mechanics, Vol. 2, Part 1, (January, 1957), pp. 33-48.

13. White, D. R.
"An Experimental Survey of the Mach Reflection of Shock Waves", Proceedings of the Second Midwestern Conference on Fluid Mechanics (Ohio State Univ. Engg. Exp. Station Bulletin #149), (1952), pp. 253-262.

14. Guderley, K. G.
"Considerations of the Structure of Mixed Subsonic-Supersonic Flow Patterns", Tech. Report No. F-TR-2168-ND, Air Materiel Command (Wright Field), (October, 1947).

15. Sternberg, J.
"Triple-Shock-Wave Intersections". The Physics of Fluids, Vol. 2, No. 2, (March-April, 1959), pp. 179-206.

16. Kawamura, R.
"On the Mach Reflection of a Shock Wave", J. of the Physical Society of Japan, Vol. 6, (1951), pp.533-534.

17. Kawamura, R., and H. Saito
"Reflection of Shock Waves - 1 Pseudo-Stationary Case", J. of the Physical Society of Japan, Vol. 11, No. 5, (May, 1956), pp. 584-592.

18. Shapiro, A. H., and S. J. Kline
"On the Thickness of Normal Shock Waves in a Perfect Gas", J. of Applied Mechanics, Vol. 21, Trans. ASME, Series E, Vol. 76, (June, 1954), pp. 185-192.

19. Seeger, R. J. and A. B. Tayler
"Triple-Shock-Wave Interactions", Physics Letters, Vol. 2, No. 7, (November, 1962), pp. 339-340.

AN INVESTIGATION OF THE TRIPLE-SHOCK-WAVE PROBLEM

by

CHARLES E. WILSON, JR.

B. S., Kansas State University, 1962

AN ABSTRACT OF A MASTER'S REPORT

submitted in partial fulfillment of the

requirements for the degree

MASTER OF SCIENCE

Department of Mechanical Engineering

KANSAS STATE UNIVERSITY

Manhattan, Kansas

1964

The intersection of three shock waves at a single point is investigated in this report. First, it is assumed that in some neighborhood of the intersection point, the shocks are straight and may be replaced by planes, disregarding any effect that shock thickness may have. Then, each shock is treated using the standard Rankine-Hugoniot theory with the boundary conditions of equal pressure and flow direction in the two regions downstream of the intersection. Several numerical solutions are performed to illustrate this so-called simple theory.

When a shock wave is incident on a rigid wall, it is found that, for all free stream Mach numbers, there is some range of incident wave angles for which a triple-shock configuration occurs. This phenomenon is called Mach reflection. Furthermore, there is a range of incident wave angles for any free stream Mach number, for which the simple theory predicts that no Mach intersection is possible. However, this gap in the theory is not matched by an experimental gap. An approximation of "isentropic" shocks used to fill the gap in the theory is discussed.

For weak incident shocks, a large discrepancy between experimental data and the simple theory appears. One possible explanation for this difference is the suspected increasing curvature of the shocks approaching the triple point. Other factors may be viscous effects and shock wave thickness. A recent paper proposes a non-Rankine-Hugoniot zone separating three Rankine-Hugoniot shocks at the point of intersection. This paper is discussed and some evaluation of the assumptions and conclusions stated therein is given in the present report.